Adv. Theor. Appl. Mech., Vol. 3, 2010, no. 8, 369 - 383

Algebraically Explicit Analytical Solution of Three-Dimensional Hyperbolic Heat Conduction Equation

Seyfolah Saedodin

Department of Mechanical Engineering, Faculty of Engineering,
Semnan University, Semnan, Iran
S_Sadodin@iust.ac.ir

Mohsen Torabi

Department of Mechanical Engineering, Faculty of Engineering
Semnan University, Semnan, Iran
Torabi_mech@yahoo.com

Abstract

In this paper, the three-dimensional hyperbolic effect subjected to a cosine heat flux boundary condition is carried out. Equations in rectangular coordinates are solved. Analytical solution with method of separation of variables is derived. The main aim of this paper is to obtain some possibly explicit analytical solution of the (1+3)-dimensional hyperbolic heat conduction equation for given initial and boundary condition with method of separation of variables. The temperature layers and profiles for various relaxation times in three different examples are calculated. Also, the reflection of the heat wave in the solid in some examples is shown.

Keywords: Hyperbolic heat conduction; Relaxation time; Separation of variables method; Heat wave reflection

1. Introduction

In the last decades, several experiments have shown that the classical theory of heat conduction in solids based on Fourier's law may fail when unsteady processes are involved. Indeed, the parabolic heat implies an infinite propagation speed of

the heat wave. Wave-like thermal response with finite propagation speed, was first observed experimentally in solid ^{4}He by Ackerman et al. [1]. In situations which include extremely high temperature gradients, extremely large heat fluxes and extremely short transient duration, the heat propagation speeds are finite. In order to obtain a theory of heat conduction, compatible with a finite propagation speed of heat wave, Cattaneo [5], and Vernotte [22] proposed a modification of Fourier's law. Which, is now well known as Cattaneo-Vernotte's constitutive equation

$$\mathbf{q} + \tau \frac{\partial \mathbf{q}}{\partial t} = -k\nabla T \tag{1}$$

Where $\mathbf{q}$ is the heat flux vector, τ is the thermal relaxation time, k is the constant thermal conductivity of the material and ∇T is the temperature gradient. If equation (1), combined with the conservation of energy gives the hyperbolic heat conduction equation

$$\frac{\partial T}{\partial t} + \tau \frac{\partial^2 T}{\partial t^2} = \alpha \Delta T \tag{2}$$

Where $\alpha = \frac{k}{\rho c}$, ρ, c and Δ are thermal diffusivity, mass density, specific heat capacity and Laplace's differential operator, respectively.

Many analytical and numerical solutions of equation (2) have been solved in the literature. Most researches applied hyperbolic heat conduction equation (HHCE), in one-dimensional. Roetzel and Das [15] and Sahoo and Roetzel [17] calculated the heat exchanger problems. Tang and Araki [20] computed the hyperbolic fin problems under the periodic thermal conditions. As well, the thin film problems are also investigated by Tan and Yang [19]. Mullis [13] discussed the rapid solidification problems. Barletta and Pulvirenti [2] have obtained the temperature field in a solid cylinder with constant as well as exponentially decaying boundary heat flux. Lor and Chu [9] analyzed the problem with the interface thermal resistance. Zhang et al. [24] processed the hyperbolic conduction model with heat source term analytically by the method of Laplace Transform. Torii and Yang [21] numerically solved the case of a thin film subjected to a symmetrical heating on both sides and Lewandowska and Malinowski [8] solved the same problem analytically by the method of the Laplace transform. Moosaie [12] investigated the hyperbolic conduction in a finite medium with the arbitrary initial conditions. Chen [7] combined the Laplace transform, weighting function scheme and the hyperbolic shape function to solve the time dependent HHCE with a conservation term. Saleh and Al-Nimr [18] employed Laplace transform, software package MATLAP and Taylor series, to solve the one-dimensional hyperbolic equation.

Few papers have been analyzed HHCE in two or three dimensions. Yang [23] developed the two-dimensional HHCE in an arbitrary body-fitted coordinate. Chen and Lin [6] formulated a numerical scheme, involving the Laplace transform technique and the control volume method for the problem. Zhou et al. [25] presented a thermal wave model of bioheat transfer, together with a seven-flux model. Saedodin and Torabi [16] investigated two-dimensional hyperbolic heat

conduction in a cylinder. To the authors' knowledge, there is only one paper that has been solved three-dimensional hyperbolic equation analytically. Barletta and Zanchini [3] analytically investigated the HHCE in three-dimensions. They applied the Laplace transform technique.

In this paper, an analytical expression of temperature field is obtained for a three-dimensional problem of the hyperbolic heat conduction. In fact, the solution of the problem is obtained by employing the method of separation of variables. Using our analytical solution, we performed sample calculation of temperature surfaces and profiles. Also, on those samples, we mention the reflection of the thermal wave.

Nomenclature

$A, B, C, a_{mk}, c_1, c_2, C_{12}, D_1, D_2, C_{nfg}$	Constant coefficients		
c	heat capacity	**Greek symbols**	
Fo	Fourier number	α	Thermal diffusivity
k	Thermal conductivity	ρ	Mass density
		Δ	Laplace's differential operator
L	Height of the solid	∇	Gradient operator
ℓ_1	Length of the solid	τ	Thermal relaxation time
ℓ_2	Width of the solid	θ	Dimensionless temperature
Ve	Vernotte number	ξ, ε, ω	Dimensionless spatial coordinates
x, y, z	Spatial coordinate	$\psi(\xi, \varepsilon, \omega, Fo)$	Function employed in Eq. (12)
$X(\xi), Y(\varepsilon), Z(\omega), T(Fo)$	Functions employed in Eq.(19)	$\phi(\xi, \varepsilon, \omega)$	Function employed in Eq. (12)
$\mathbf{q}$	Heat flux vector		
t	Temporal coordinate	$\beta_m, \gamma_k, \lambda_n, \eta_f, \mu_g$	Eigenvalues
T	Temperature	κ	Parameter defined by Eq. (35a)
T_∞	Ambient temperature	κ_i	Parameter defined by Eq. (35b)
T_i	Initial temperature	ϑ_l	Parameter defined by Eq. (33)

2. Problem statement

There are many kinds of heat flux boundary conditions in natural and technology. For heat flux, Mirahmadi et al. [10] utilized Gaussian distribution heat flux. Moosaie [11] utilized the time-dependence cosine heat flux. In this paper, we

utilized space-dependence cosine function as a heat flux boundary condition in one of the six boundary surfaces.

2.1. Governing differential equation

Consider a solid, as shown as Fig. 1. For this case, a three-dimensional unsteady HHCE without any heat generation can then be expressed as:

$$\frac{\partial T}{\partial t}+\tau\frac{\partial^2 T}{\partial t^2}=\alpha\left(\frac{\partial^2 T}{\partial x^2}+\frac{\partial^2 T}{\partial y^2}+\frac{\partial^2 T}{\partial z^2}\right) \tag{3}$$

2.2. Boundary conditions

For this case the boundary conditions are:

$$\frac{\partial}{\partial x}T(0,y,z,t)=0 \tag{4a}$$

$$T(\ell_1,y,z,t)=T_\infty \tag{4b}$$

$$\frac{\partial}{\partial y}T(x,0,z,t)=0 \tag{4c}$$

$$T(x,\ell_2,z,t)=T_\infty \tag{4d}$$

$$T(x,y,0,t)=T_\infty \tag{4e}$$

$$k\frac{\partial}{\partial z}T(x,y,L,t)=q\cos\left(\frac{x}{\ell_1}\right)\cos\left(\frac{y}{\ell_2}\right) \tag{4f}$$

2.3. Initial conditions

Consider the solid initially has been at the ambient temperature. Then:

$$T_i=T_\infty \tag{5}$$

Hence the initial conditions are:

$$T(x,y,z,0)=T_\infty \tag{6a}$$

$$\frac{\partial}{\partial t}T(x,y,z,0)=0 \tag{6b}$$

3. Analytical solution

We introduce the following dimensionless quantities:

$$\theta = k\frac{T-T_\infty}{Lq}, \qquad \xi = \frac{x}{\ell_1}, \qquad \varepsilon = \frac{y}{\ell_2}, \qquad \omega = \frac{z}{L}, \qquad Fo = \frac{\alpha t}{L^2}, \qquad Ve = \sqrt{\frac{\alpha\tau}{L^2}} \tag{7}$$

Where θ is dimensionless temperature and ξ, ε, ω are dimensionless coordinates. Fo is the Fourier number, Ve is the Vernotte number. In our treatment, we assume:

$$\ell_1 = \ell_2 = L \tag{8}$$

By introducing the dimensionless quantities and Eq. (8), we expressed HHCE as:

$$Ve^2\frac{\partial^2\theta}{\partial Fo^2} + \frac{\partial\theta}{\partial Fo} = \frac{\partial^2\theta}{\partial\xi^2} + \frac{\partial^2\theta}{\partial\varepsilon^2} + \frac{\partial^2\theta}{\partial\omega^2} \tag{9}$$

Also, the boundary conditions are:

$$\frac{\partial}{\partial\xi}\theta(0,\varepsilon,\omega,Fo) = 0 \tag{10a}$$

$$\theta(1,\varepsilon,\omega,Fo) = 0 \tag{10b}$$

$$\frac{\partial}{\partial\varepsilon}\theta(\xi,0,\omega,Fo) = 0 \tag{10c}$$

$$\theta(\xi,1,\omega,Fo) = 0 \tag{10d}$$

$$\theta(\xi,\varepsilon,0,Fo) = 0 \tag{10e}$$

$$\frac{\partial}{\partial\omega}\theta(\xi,\varepsilon,1,Fo) = \cos(\xi)\cos(\varepsilon) \tag{10f}$$

and the initial conditions are:

$$\theta(\xi,\varepsilon,\omega,0) = 0 \tag{11a}$$

$$\frac{\partial}{\partial Fo}\theta(\xi,\varepsilon,\omega,0) = 0 \tag{11b}$$

If we want to apply the separation of variables method, first we should split up eq. (9) into a set of simpler problems. Carslaw and Jaeger [4] and Özisik [14] determined the solution of Eq. (9) from:

$$\theta(\xi,\varepsilon,\omega,Fo) = \psi(\xi,\varepsilon,\omega,Fo) + \phi(\xi,\varepsilon,\omega) \tag{12}$$

Where the temperature $\phi(\xi,\varepsilon,\omega)$ is taken as the solution of the following Eqs.:

$$\frac{\partial^2\phi}{\partial\xi^2}+\frac{\partial^2\phi}{\partial\varepsilon^2}+\frac{\partial^2\phi}{\partial\omega^2}=0 \tag{13}$$

$$\frac{\partial}{\partial\xi}\phi(0,\varepsilon,\omega)=0 \tag{14a}$$

$$\phi(1,\varepsilon,\omega)=0 \tag{14b}$$

$$\frac{\partial}{\partial\varepsilon}\phi(\xi,0,\omega)=0 \tag{14c}$$

$$\phi(\xi,1,\omega)=0 \tag{14d}$$

$$\phi(\xi,\varepsilon,0)=0 \tag{14e}$$

$$\frac{\partial}{\partial\omega}\phi(\xi,\varepsilon,1)=\cos(\xi)\cos(\varepsilon) \tag{14f}$$

Where the temperature $\psi(\xi,\varepsilon,\omega,Fo)$ is taken as the solution of the following Eqs.:

$$Ve^2\frac{\partial^2\psi}{\partial Fo^2}+\frac{\partial\psi}{\partial Fo}=\frac{\partial^2\psi}{\partial\xi^2}+\frac{\partial^2\psi}{\partial\varepsilon^2}+\frac{\partial^2\psi}{\partial\omega^2} \tag{15}$$

$$\frac{\partial}{\partial\xi}\psi(0,\varepsilon,\omega,Fo)=0 \tag{16a}$$

$$\psi(1,\varepsilon,\omega,Fo)=0 \tag{16b}$$

$$\frac{\partial}{\partial\varepsilon}\psi(\xi,0,\omega,Fo)=0 \tag{16c}$$

$$\psi(\xi,1,\omega,Fo)=0 \tag{16d}$$

$$\psi(\xi,\varepsilon,0,Fo)=0 \tag{16e}$$

$$\frac{\partial}{\partial\omega}\psi(\xi,\varepsilon,1,Fo)=0 \tag{16f}$$

$$\psi(\xi,\varepsilon,\omega,0)=-\phi(\xi,\varepsilon,\omega) \tag{16g}$$

$$\frac{\partial}{\partial Fo}\psi(\xi,\varepsilon,\omega,0)=0 \tag{16h}$$

The solution of the partial differential equation (13) becomes

$$\phi(\xi,\varepsilon,\omega)=\sum_{m=0}^{\infty}\sum_{k=0}^{\infty}[a_{mk}\cos(\beta_m\xi)\cos(\gamma_k\varepsilon)\sinh(\omega\sqrt{\beta_m{}^2+\gamma_k{}^2})] \tag{17}$$

Where β_m and γ_k are eigenvalues of Eqs. $\cos\beta_m=0$ and $\cos\gamma_k=0$, respectively. Using boundary condition (14f) and Utilizing orthogonality condition, the constant a_{mk} is given as following Eq.:

$$a_{mk} = \frac{1}{\sqrt{\beta_m{}^2 + \gamma_k{}^2}\cosh(\sqrt{\beta_m{}^2 + \gamma_k{}^2})} \times \left[\frac{\sin(1+\beta_m)}{1+\beta_m} + \frac{\sin(1-\beta_m)}{1-\beta_m}\right] \times \left[\frac{\sin(1+\gamma_k)}{1+\gamma_k} + \frac{\sin(1-\gamma_k)}{1-\gamma_k}\right] \tag{18}$$

To solve the partial differential equation (15), we should use the following separation ansantz:

$$\psi(\xi,\varepsilon,\omega,Fo) \equiv X(\xi)Y(\varepsilon)Z(\omega)T(Fo) \tag{19}$$

By substituting the Eq. (19) into the Eq. (15) and subtracting to (19):

$$-(Ve^2\frac{1}{T}\frac{d^2T}{dFo^2} + \frac{1}{T}\frac{dT}{dFo}) + \frac{1}{X}\frac{d^2X}{d\xi^2} + \frac{1}{Y}\frac{d^2Y}{d\varepsilon^2} + \frac{1}{Z}\frac{d^2Z}{d\omega^2} = \pm\lambda^2 \tag{20}$$

Here $+\lambda^2$ is suitable to our problem. Finally, the problem separately expressed in ξ- and ε- and ω- and Fo-directions as follows:

$$\frac{d^2X}{d\xi^2} + \lambda^2 X = 0 \tag{21}$$

$$\frac{d}{d\xi}X(0) = 0 \tag{22a}$$

$$X(1) = 0 \tag{22b}$$

$$\frac{d^2Y}{d\varepsilon^2} + \eta^2 Y = 0 \tag{23}$$

$$\frac{d}{d\varepsilon}Y(0) = 0 \tag{24a}$$

$$Y(1) = 0 \tag{24b}$$

$$\frac{d^2Z}{d\omega^2} + \mu^2 Z = 0 \tag{25}$$

$$Z(0) = 0 \tag{26a}$$

$$\frac{d}{d\omega}Z(1) = 0 \tag{26b}$$

$$Ve^2\frac{d^2T}{dFo^2} + \frac{dT}{dFo} + (\lambda^2 + \eta^2 + \mu^2)T = 0 \tag{27}$$

$$\frac{d}{dFo}T(0) = 0 \tag{28}$$

Solving the Eqs. (21), (23) and (25) we obtain:

$$X(\xi) = A\cos(\lambda_n\xi) \tag{29}$$

$$Y(\varepsilon) = B\cos(\eta_f\varepsilon) \tag{30}$$

$$Z(\omega) = C\sin(\mu_g\omega) \tag{31}$$

Where λ_n, η_f and μ_g are eigenvalues of Eqs. $\cos\lambda_n = 0$, $\cos\eta_f = 0$ and $\cos\mu_g = 0$, respectively. For the Eq. (27), if $1-4Ve^2\vartheta_l{}^2 > 0$, we obtain:

$$T(Fo) = e^{-\frac{Fo}{2Ve^2}}(c_1\sinh(\frac{\kappa Fo}{2Ve^2}) + c_2\cosh(\frac{\kappa Fo}{2Ve^2})) \tag{32}$$

Where

$$\vartheta_l{}^2 = \lambda_n{}^2 + \eta_f{}^2 + \mu_g{}^2 \tag{33}$$

And if $1-4Ve^2\vartheta_l{}^2 < 0$

$$T(Fo) = e^{-\frac{Fo}{2Ve^2}}\left(c_1 \sin\left(\frac{\kappa_i Fo}{2Ve^2}\right) + c_2 \cos\left(\frac{\kappa_i Fo}{2Ve^2}\right)\right) \tag{34}$$

Where

$$\kappa = \sqrt{1-4Ve^2\vartheta_l{}^2} \tag{35a}$$

$$\kappa = i\kappa_i \tag{35b}$$

By substituting the Eqs. (32) and (34) into initial condition (28) to eliminating c_1 or c_2:

$$T(Fo) = C_{12}\begin{cases} e^{-\frac{Fo}{2Ve^2}}\left\{\frac{1}{\kappa}\sinh\left(\frac{\kappa Fo}{2Ve^2}\right) + \cosh\left(\frac{\kappa Fo}{2Ve^2}\right)\right\} & \kappa = real \\ e^{-\frac{Fo}{2Ve^2}}\left\{\frac{1}{\kappa_i}\sin\left(\frac{\kappa_i Fo}{2Ve^2}\right) + \cos\left(\frac{\kappa_i Fo}{2Ve^2}\right)\right\} & \kappa = i\kappa_i \end{cases} \tag{36}$$

Substituting the Eqs. (29-31) and (36) into (19), the following equation for $\psi(\xi,\varepsilon,\omega,Fo)$ obtain:

$$\psi(\xi,\varepsilon,\omega,Fo) = \sum_{n=0}^{N}\sum_{f=0}^{F}\sum_{g=0}^{G} C_{nfg}\exp\left(-\frac{Fo}{2Ve^2}\right)\times\left[\frac{1}{\kappa}\sinh\left(\frac{\kappa Fo}{2Ve^2}\right) + \cosh\left(\frac{\kappa Fo}{2Ve^2}\right)\right]$$
$$\times\cos(\lambda_n\xi)\cos(\eta_f\varepsilon)\sin(\mu_g\omega) \tag{37}$$
$$+\sum_{N+1}^{\infty}\sum_{F+1}^{\infty}\sum_{G+1}^{\infty} C_{nfg}\exp\left(-\frac{Fo}{2Ve^2}\right)\left[\frac{1}{\kappa_i}\sin\left(\frac{\kappa_i Fo}{2Ve^2}\right) + \cos\left(\frac{\kappa_i Fo}{2Ve^2}\right)\right]\times\cos(\lambda_n\xi)\cos(\eta_f\varepsilon)\sin(\mu_g\omega)$$

Where N,F,G are maximum value of n,f,g when the κ is real for each loop, respectively. Finally, using the Eq. (16g) and orthogonality condition

$$C_{nfg} = -2\left[\frac{\sin(1+\lambda_n)}{1+\lambda_n} + \frac{\sin(1-\lambda_n)}{1-\lambda_n}\right]\times\left[\frac{\sin(1+\eta_f)}{1+\eta_f} + \frac{\sin(1-\eta_f)}{1-\eta_f}\right]\frac{(-1)^g}{\lambda_n{}^2 + \eta_f{}^2 + \mu_g{}^2} \tag{38}$$

As a good comparison, we should solve the three-dimensional parabolic equation. If Fourier's law holds, i.e. in the limit $Ve \to 0$, the values of κ_i are always real and therefore, $\psi(X,T,Z,Fo)$ becomes

$$\psi(\xi,\varepsilon,\omega,Fo) = \sum_{n=0}^{\infty}\sum_{f=0}^{\infty}\sum_{g=0}^{\infty} C_{nfg}\exp(-\vartheta_l{}^2 Fo)\cos(\lambda_n\xi)\cos(\eta_f\varepsilon)\sin(\mu_g\omega) \tag{39}$$

4. Result and discussion

Using our analytical solution, we performed sample calculations of temperature surfaces and profiles, based on Eqs. (12), (17), (37) and (39). The results of calculations are presented in Figs. 2-5.

4.1. Comparison of surface temperature evolvement obtained from Fourier and non-Fourier model with same Fourier number

Fig. 2 shows the surface temperature profiles for the two cases. The Fourier number and ε that we simulated for are 0.4 and zero, respectively. It can be perceived from Fig. 2a that, in Fourier model the speed of propagation is infinite.Hence, all of the solid can touch the heat flux. But it can be perceived from Figs. 2b and 2c that, because of the non-Fourier effect, the heat wave cannot touch the other side of the solid at the moment. In addition, it can be seen that, if the Vernotte number increases, the traverse distance of the heat wave decreases. Furthermore, Fig. 2 shows that, the more Vernotte number, the less thermal penetration depth.

4.2. Comparison of temperature distribution for non-Fourier model with same Fourier number but at different Vernotte number along the ω direction

Fig. 3 shows temperature profiles along the ω direction at $Fo = 0.4$, $\xi = \varepsilon = 0.5$. It can be seen from Fig. 3 that, while Vernotte number is bigger than Fourier number, there are many points that don't feel the effect of heat flux. It can be seen that, until the heat flux dosen't touch the other side of the solid, while the Vernotte number increases, the dimensionless temperature decreases. But after the heat flux touches the other side of the solid, if the Vernotte number increases, the dimensionless temperature is decreases.

4.3. Comparison of temperature distribution for the non-Fourier model with different Vernotte number for the unique point

Fig. 4 shows temperature profiles at the point $\xi = \varepsilon = \omega = 0.5$. It can be seen from Fig. 4 that, the higher Vernotte number causes each point to be at initial temperature, more. Moreover, it can be perceived again from Fig. 4 that, as much as the Vernotte number is higher, the point can get to higher temperature during the process. Also the thermal wave reflection, causes the existence of a fracture in the thermal profile of the point. In the Fig. 5, the fracture of the thermal wave can be observed, for the two Vernotte numbers, 0.3 and 0.5. As can be observed in the Fig. 5, the reflective wave with the Vernotte number 0.5, could touch and pass the point. Therefore, the temperature profile fracture can be seen in the Fig. 4, for this Vernotte number. But for the Vernotte number 0.7, the reflective wave cannot touch the point till $Fo = 1$. Hence in Fig. 4, any fracture cannot be observed in the temperature profile.

5. Conclusion

In this paper, the three-dimensional HHCE was solved analytically with the space-dependence cosine boundary condition by the separation of variables method. We perceived that, the more the Vernotte number, the more the Fourier number needed for the solid to reach an equilibrium temperature. In addition we

investigated the wave reflection and we observed that due to the difference of a Vernotte number in a particular Fourier number, the wave reflection can reach the considered point, pass that or before reaching this point, the wave reflection occurs in the solid and propagates in the solid.

Acknowledgment

The authors would like to acknowledge the support of the department of mechanical engineering and the office of gifted of Semnan University for funding the current research grant.

References

[1] C.C. Ackerman, B. Berman, H.A. Fairbank and R.A. Guyer, Second sound in solid helium, Phys. Rev. Lett. 16 (1966) 789–791.

[2] A. Barletta and B. Pulvirenti, Hyperbolic thermal waves in a solid cylinder with a non-stationary boundary heat flux, Int. J. Heat Mass Transf.41 (1998) 107–116.

[3] A. Barletta and E. Zanchini, Three-dimensional propagation of hyperbolic thermal waves in a solid bar with rectangular cross-section, Int. J. Heat Mass Transf.42 (1999) 219-229.

[4] H. S. Carslaw and J. C. Jaeger, Conduction of Heat in Solids, 2nd ed., Oxford University Press, New York, 2000.

[5] C. Cattaneo, Sur une forme de l'équation de la chaleur éliminant le paradoxe d'une propagation instantanée, C.R. Acad. Sci. 247 (1958) 431–433.

[6] H.T. Chen and J. Y. Lin, Analysis of two-dimensional hyperbolic heat conduction problems, Int. J. Heat Mass Transf.37 (1993) 153–164.

[7] T.M. Chen, Numerical solution of hyperbolic heat conduction in thin surface layers, Int. J. Heat Mass Transf.50 (2007) 4424–4429.

[8] M. Lewandowska and L. Malinowski, An analytical solution of the hyperbolic heat conduction equation for the case of a finite medium symmetrically heated on both sides, Int. Commun. Heat Mass Transf. 33 (2006) 61–69.

[9] W.B. Lor and H.S. Chu, Effect of interface thermal resistance on heat transfer in a composite medium using the thermal wave model, Int. J. Heat Mass Transf.43 (2000) 653–663.

[10] A. Mirahmadi, S. Saedodin and Y. Shanjani, Numerical Heat Transfer Modeling in Coated Powder as Raw Material of Powder-Based Rapid Prototyping Subjected to Plasma Arc, Numer. Heat Transf. Part A 51 (2007) 593–613.

[11] A. Moosaie, Non-Fourier heat conduction in a finite medium subjected to arbitrary periodic surface disturbance, Int. Commun. Heat Mass Transf. 34 (2007) 996–1002.

[12] A. Moosaie, Non-Fourier heat conduction in a finite medium with insulated boundaries and arbitrary initial conditions, Int. Commun. Heat Mass Transf.35 (2008) 103–111.

[13] A. M. Mullis, Rapid solidification within the framework of a hyperbolic conduction model, Int. J. Heat Mass Transf.40 (1997) 4085–4094.

[14] M. N. Ozisik, Heat conduction, 2nd ed., John Wiley &Sons, New York, 1993.

[15] W. Roetzel and S. K. Das, Hyperbolic axial dispersion model: concept and its application to a plate heat exchanger, Int. J. Heat Mass Transf.38 (1995) 3065–3076.

[16] S. Saedodin and M. Torabi, Analytical Solution of Non-Fourier Heat Conduction in Cylindrical Coordinates, Int. Rev. of Mech. Eng. 3 (2009), 726-732.

[17] R. K. Sahoo and W. Roetzel, Hyperbolic axial dispersion model for heat exchangers, Int. J. Heat Mass Transf.45 (2002) 1261–1270.

[18] A. Saleh and M. Al-Nimr, Variational formulation of hyperbolic heat conduction problems applying Laplace transform technique, Int. Commun. Heat Mass Transf.35 (2008) 204–214.

[19] Z.M. Tan and W.J. Yang, Heat transfer during asymmetrical collision of thermal waves in a thin film, Int. J. Heat Mass Transf.40 (1997) 3999–4006.

[20] D.W. Tang and N. Araki, Non-Fourier heat conduction in a finite medium under periodic surface thermal disturbance, Int. J. Heat Mass Transf. 39 (1996) 1585–1590.

[21] S. Torii and W. J. Yang, Heat transfer mechanisms in thin film with laser heat source, Int. J. Heat Mass Transf. 48 (2005) 537–544.

[22] P. Vernotte, Les paradoxes de la théorie continue de l'équation de la chaleur, C.R. Acad. Sci. 246 (1958) 3154–3155.

[23] H.Q. Yang, Solution of two-dimensional hyperbolic heat conduction by high-resolution numerical method, Numer. Heat Transf. Part A 21 (1992) 333–349.

[24] D. Zhang, L. Li, Z. Li, L. Guan and X. Tan, Non-Fourier conduction model with thermal source term of ultra short high power pulsed laser ablation and temperature evolvement before melting, Physica B 364 (2005) 285–293.

[25] J. Zhou, Y. Zhang and J. K. Chen, Non-Fourier Heat Conduction Effect on Laser-Induced Thermal Damage in Biological Tissues, Numer. Heat Transf. Part A 54 (2008) 1–19.

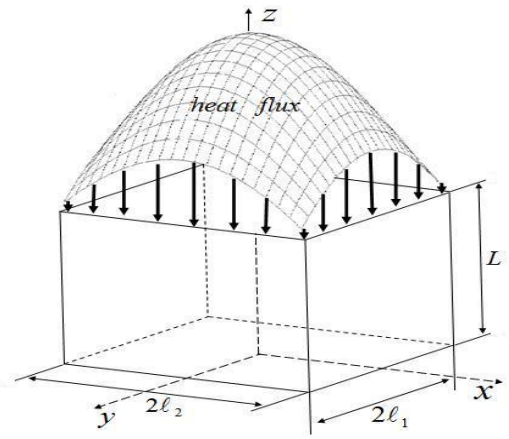

Fig. 1. The solid configuration

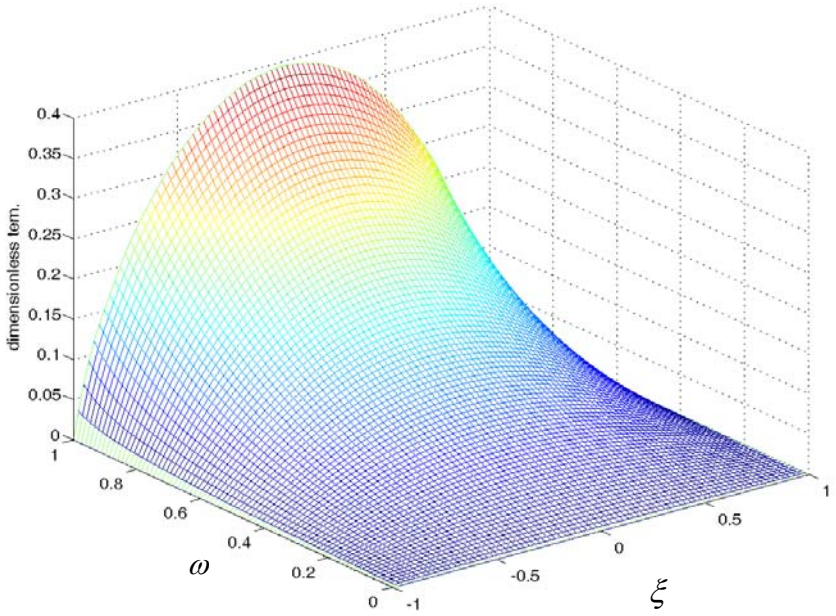

(a)

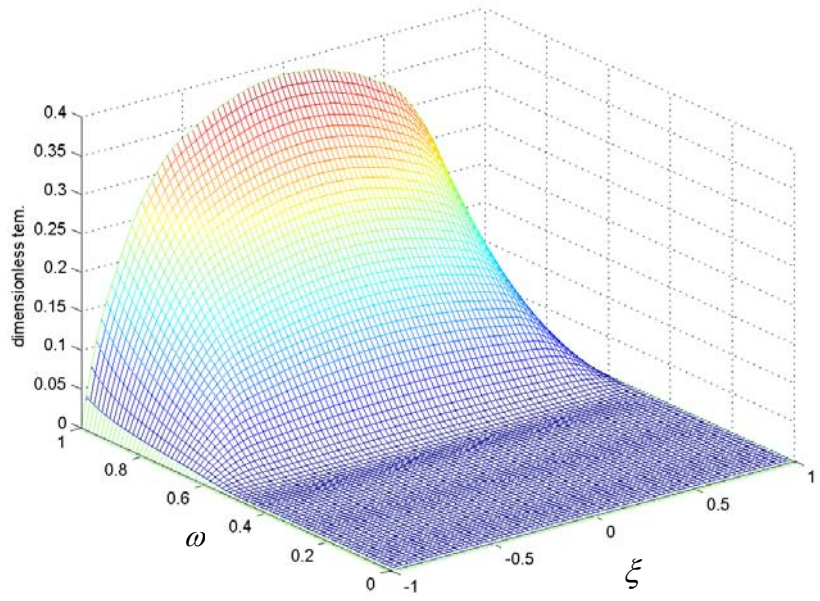

(b)

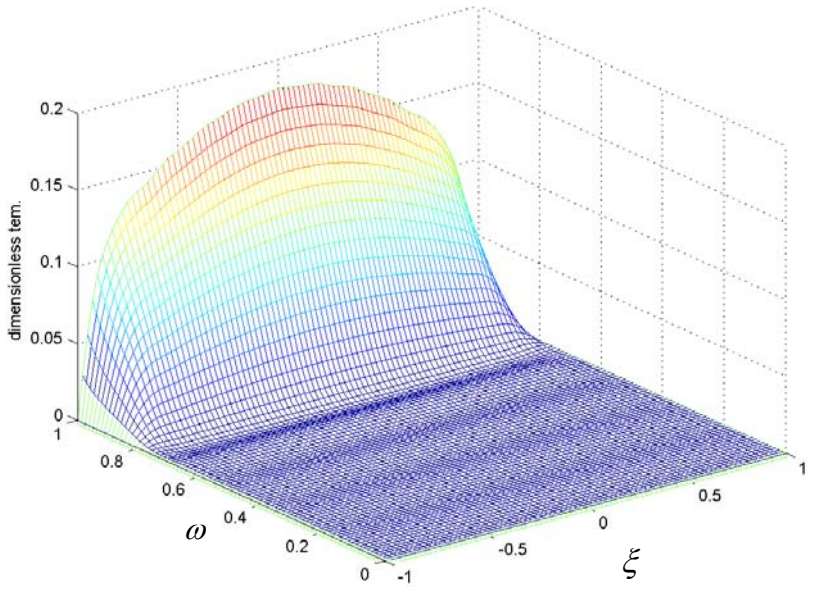

(c)

Fig.2. The surface temperature evolution with $Fo = 0.4$ for different Vernotte number (a) Fourier model ($Ve = 0$) (b) $Ve = 0.7$ (c) $Ve = 0.9$

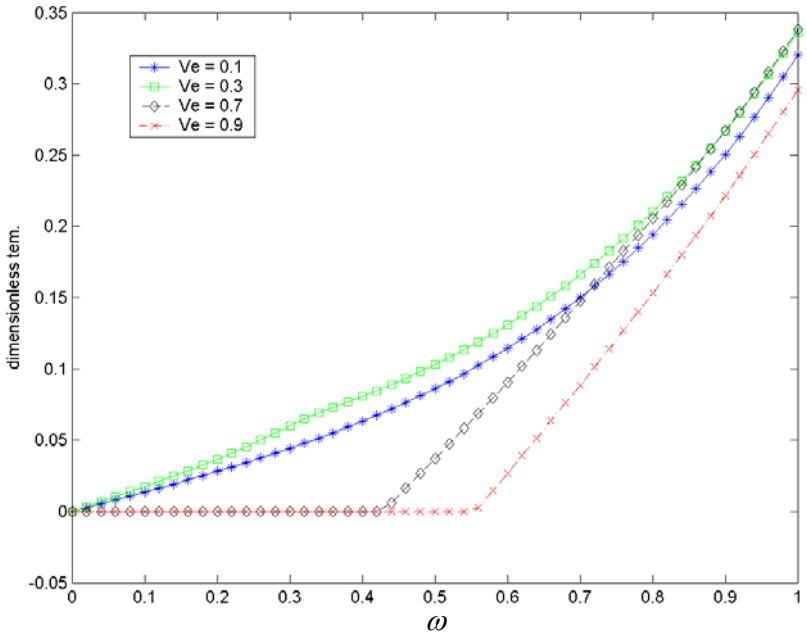

Fig.3. The distribution for the non-Fourier model with the same Fourier number, but at different Vernotte number along the ω direction

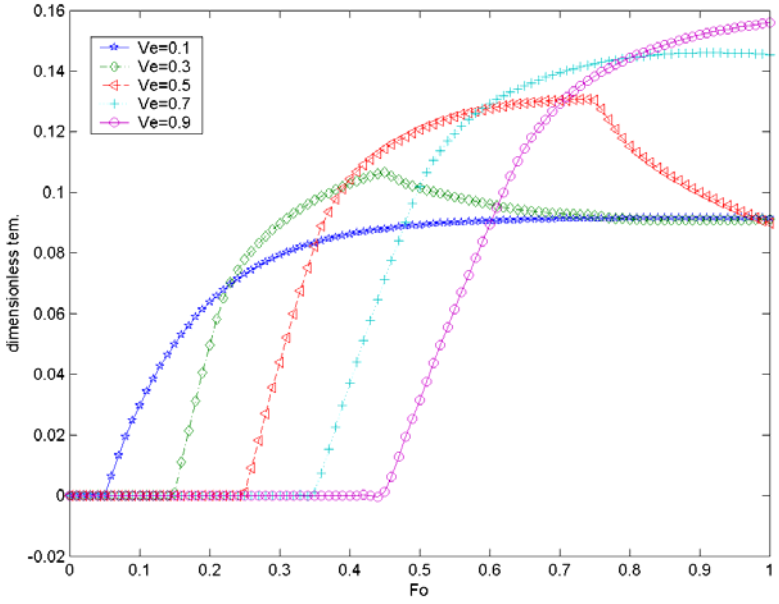

Fig. 4. The temperature distribution for non-Fourier model with different Vernotte number for the unique point

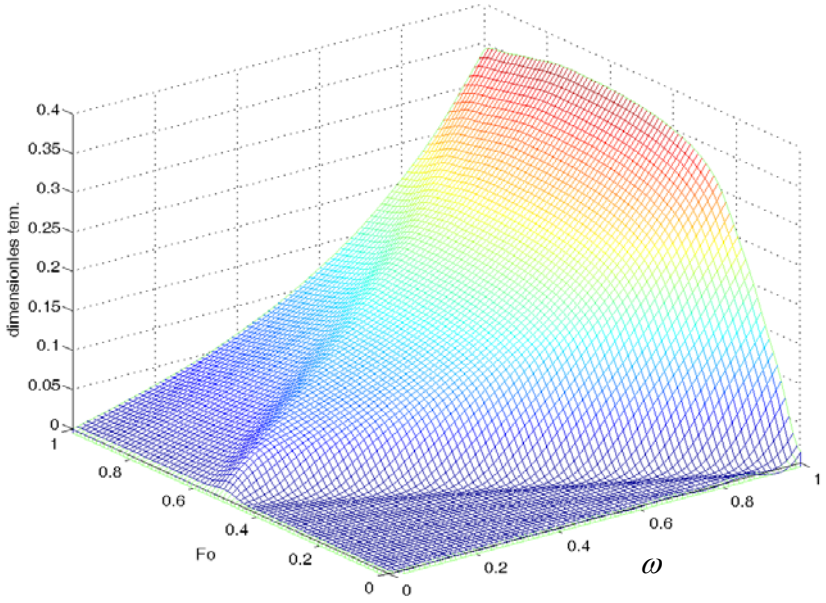

(a)

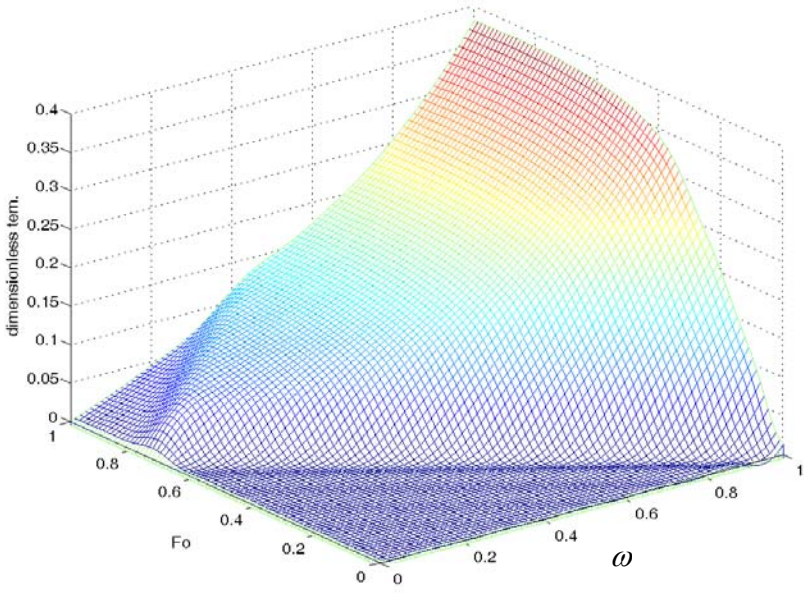

(b)

Fig. 5. The surface temperature evolution and reflection of the heat wave at $\xi = \varepsilon = 0.5$ for different Vernotte number (a) $Ve = 0.5$ (b) $Ve = 0.7$

Received: May, 2010